OUTER LIMITS AND INNER STRUCTURE:
THE 3-DIMENSIONAL FLOW FIELD OF
PLEUROMAMMA XIPHIAS (CALANOIDA: METRIDINIDAE)

David Fields and Jeannette Yen

ABSTRACT

Copepods create feeding currents to entrain water over their sensory receptors and through their feeding appendages. The flow field also creates a hydrodynamic disturbance which may be detected by the animal's potential prey and predators. A method is described for the 3-dimensional analysis of the flow field of feeding copepods. The equipment used is a laser-illuminated flow visualization system and video recordings made from 2 perpendicularly mounted cameras which permitted the determination of the X, Y and Z coordinates of individual particles and their trajectories. Flow within narrow volumes of water are used to minimize the error in flow rate estimates associated with analysying flow within a large unspecified volume of water compressed into a 2-dimensional plane. Three planar views are combined to create a 3-dimensional model describing the shape and magnitude of the flow field of *Pleuromamma xiphias*. A maximum velocity of 38.00 mm·s^{-1} occurred at the base of the downward swing of 2nd antennae just lateral to the sides of the body. We found lateral symmetry in the flow field with water velocity decreasing exponentially from the head to the distal tips of the antennae exposing different parts of the sensor to different flow regimes. Asymmetry in the flow field was found between the dorsal and ventral side of the animal with the 1.00 mm·s^{-1} velocity isoline approximately 1.5 times further from the body ventrally than dorsally. The asymmetry between the dorsal and ventral flow is predominantly within the region of low flow, therefore there is relatively little difference in the amount of water entrained from each side. However, because the escape responses of mechanoreceptive prey may be elicited by steep velocity gradients, the asymmetry may allow prey to be entrained closer ventral than dorsal to the animal. The hydrodynamic disturbance defined by the 1.00 mm·s^{-1} velocity isoline was detected as far as 4.10 mm above the head, 4.60 mm lateral, 5.60 mm ventral and 3.60 mm dorsal to the animal. The lower extent of the 1.00 mm·s^{-1} isoline was not detected however the lower portion of the 7.00 mm·s^{-1} isoline was found 7.50 mm directly below the head. Using the above dimensions and a spheroid model, the volume of the hydrodynamic disturbance created by the animal (approximately 4 ml) is greater than 175 times the actual volume of the physical body of the animal. This created signal may reveal the identity and location of *Pleuromamma xiphias* to its predators.

The entrainment of water by copepods over their sensors, most important of which are the first antennae, and the feeding appendages has been qualitatively described in the literature (Cannon, 1928; Strickler, 1985). Strickler (1985) hypothesized that the function of the generated flow field is to both enable the animal to scan large quantities of water, using either mechano- or chemoreception (or both), and to maximize the amount of fluid which passes through its feeding appendages. However, the flow field also creates a hydrodynamic disturbance which may be sensed by both an animal's prey and predators.

Recent literature has shown that the fine scale structure of the generated flow field may have strong implications for the manner by which copepods capture rheotactic food (Yen and Fields, 1992; Tiselius and Jonsson, 1990) and detect potential predators (Lenz and Yen, 1993). Yen and Fields (1992) reported that localized gradients in water velocities (giving rise to shear stress) elicited escape responses in *Acartia tonsa* nauplii from the flow field of *Temora longicornis*. Similar responses to fluid deformations were found for the copepod *Calanus*

finmarchicus (Haury et al., 1980) and the rotifer *Keratella* spp. (Gilbert and Kirk, 1988), although the shear stress associated with the escape response of each type of animal was different. Therefore, the structure of the predator's flow field and the orientation of the prey's sensors, within both its own flow field and that of the predator, can determine whether a potential prey detects its predator prior to entering its capture region. From the perspective of the predators, copepods also must be able to assess the size and location of their prey. Strickler and Twombly (1975) suggest that swimming copepods can be characterized by their particular fluid dynamic disturbance. The predator and the prey may therefore be assessing the morphology of the flow field itself rather than the morphology defined by the physical body of the prey and predator respectively (Strickler, 1985).

Historically, particle trajectories and flow field analysis of animals which generate feeding currents have been done by analysing flow within an unspecified 3-dimensional volume compressed onto a 2-dimensional plane. In doing this, an appreciation for the fine scale structure of the flow field was lost. Without the structure, the relationship between the flow field and the feeding ecology of copepods could not be developed. Describing and quantifying the shape and magnitude of the hydrodynamic disturbance is essential to the understanding of predator-prey interaction between aquatic mechanoreceptive organisms.

The objective of our study is to characterize the flow field of *Pleuromamma xiphias,* an omnivorous (Mullin, 1966; Bennett and Hopkins, 1989), bioluminescent (Buskey et al., 1989), vertically migrating (Ambler and Miller, 1987; Haury, 1988) calanoid copepod. *P. xiphias* has been shown to be a preferred diet for mid-water nekton (Hopkins and Baird, 1981, 1985), euphausiids (Hu, 1978), and decapods (Foxton and Roe, 1974). Its own diet includes diatoms, dinoflagellates and smaller crustaceans (Bennett and Hopkins, 1989). In addition, we present a method that describes and quantifies the hydrodynamic disturbance generated by flow producing animals.

METHODS

Pleuromamma xiphias (3.5 mm prosome length) were collected from 600 m off the island of Hawaii, Hawaii, pumped through a 40-in diameter, 0.5-mi.-long pipe (Ocean Thermal Energy Conversion facility of the Natural Energy Laboratory of Hawaii; Kitalong, 1988). A single, low power, He-Ne laser (632.8 nm) with a split beam illuminates two perpendicularly mounted video cameras (Pulnix TM-745) which permits determinations of X, Y, Z co-ordinates or locations in 3-dimensional space (Yen and Fields, 1992; Strickler, 1985). Camera shutter speed was set at $\frac{1}{2000}$th sec to minimize blurring of the particles. All animals used in the present analysis were tethered to 38 gauge (0.0038 in) tin electrical wire and suspended in 100 ml of filtered sea water at 21°C. Temporal resolution in the analysis was $\frac{1}{30}$ of a sec. This resolution was too slow to resolve the effects of the individual beats of the feeding current appendages, therefore the water velocities reported are averaged over the entire beat frequency.

A velocity contour of the animal's flow field was constructed by filming the animal from the two perpendicular views at three different polar coordinates. To orient the animal for the three different polar coordinates the tether of the animal was attached to a post mounted with a protractor. The degree of rotation could be changed and measured with only a minimum of disturbance to the animal. Assuming a polar coordinate of 0 degrees when the animal was being filmed from the dorsal view on one camera and a lateral view from the left side, a video was made of the 0, 45 and 90 degree angles (Fig. 1). At each polar coordinate a Cartesian coordinate system was used to plot particle trajectories. One camera was used for the X Z co-ordinates while the Y Z coordinates were taken from the other camera (Strickler, 1985). To represent the volume of water entrained in the flow field as a two dimensional plane, a narrow corridor of water, 1.25 mm wide, was defined in one of the camera views (Fig. 2). Particle matching was accomplished by comparing the downward velocity component (Z) of each particle trajectory in the two perpendicular views. To minimize the number of particles occupying the same Z position at any one time, low concentrations of particles (800 particles/mL) were used. By plotting only the trajectories of particles which remained within this corridor for a distance of at least a body length, the lateral component of each of the particle trajectories could be treated as
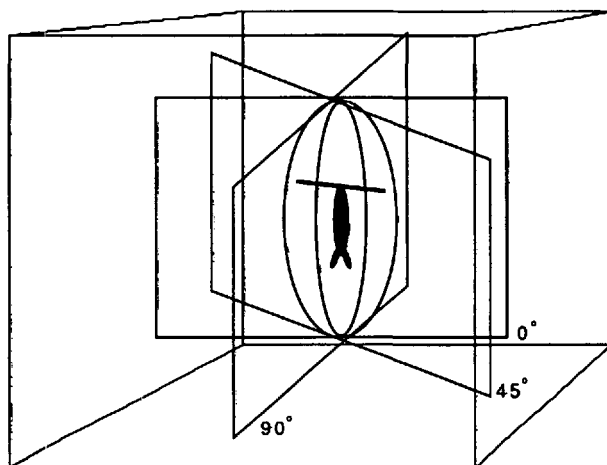
Figure 1.   Three planes in which particle trajectories for *Pleuromamma xiphias* were mapped.

negligible (possible 4% underestimation). A total of 105 different particle trajectories were mapped encompassing over 1300 X Z or Y Z data points. To test for temporal stability and the stability of the flow field between animals of the same sex and age class, particle trajectories above the antennae were recorded for three different animals. Once mapped, the velocity was calculated as the distance traveled over a measured time interval and a two dimensional Cartesian coordinate was assigned to the midpoint of the velocity vector. To diminish the error associated with assigning the magnitude of the velocity to the mid-point of large velocity vectors, different time scales were used depending on the distance traveled. For those water velocities slower than 1.00 mm$\cdot$s^{-1}, $\frac{1}{3}$ of a sec was used, from 1.00 mm$\cdot$s^{-1} to 3.50 mm$\cdot$s^{-1}, and over 3.50 mm$\cdot$s^{-1}, the distance traveled over $\frac{1}{6}$ and $\frac{1}{30}$ of a sec, respectively, were used. Water velocity was assumed to be adequately represented by the speed and trajectories of the 20-μm polystyrene spheres which were used as tracers for the water flow velocity (Polyscience). The Cartesian coordinates from each of the three different views were analyzed using the contouring software package SURFER located on a GATEWAY 386-33 computer.

RESULTS

Feeding Current Appendages. — The flow field is created primarily through the beating motion of the 2nd antennae. However a continuous "fling and clap" (Koehl and Strickler, 1981) motion was also observed in the 2nd maxilla. Present equipment only permitted resolution of $\frac{1}{30}$ of a sec in frame by frame analysis. At this resolution beat frequency could not be determined.

Above the Antennae. — Defined by the velocity isopleths, the structure of the feeding current above the first antennae from the dorsal view of the animal (Fig. 3A) can be roughly described as concentric arcs with the centers near the head of the animal. The integrity of the created hydrodynamic disturbance from this perspective remained intact to the distal tips of the antennae and 4.10 mm above the head. The highest velocity in this region, 10.30 mm$\cdot$s^{-1}, was measured directly above the first antennae at approximately 0.47 mm from the head on the right-hand side. In general, however, left and right symmetry was found (Figs. 3A, 4, 6). Particle trajectories (Fig. 3B, D, F) above the first antennae show acceleration toward the mid-point of the body. Particle trajectories were found not to cross each other, even as they converged in the regions with the highest velocity closest to the body. This indicates laminar flow throughout the region above the antennae. Water velocity decreased exponentially along the first antennae (Fig. 4). At the distal tips of the antennae, the water velocity measured as low as $\frac{1}{10}$ the value
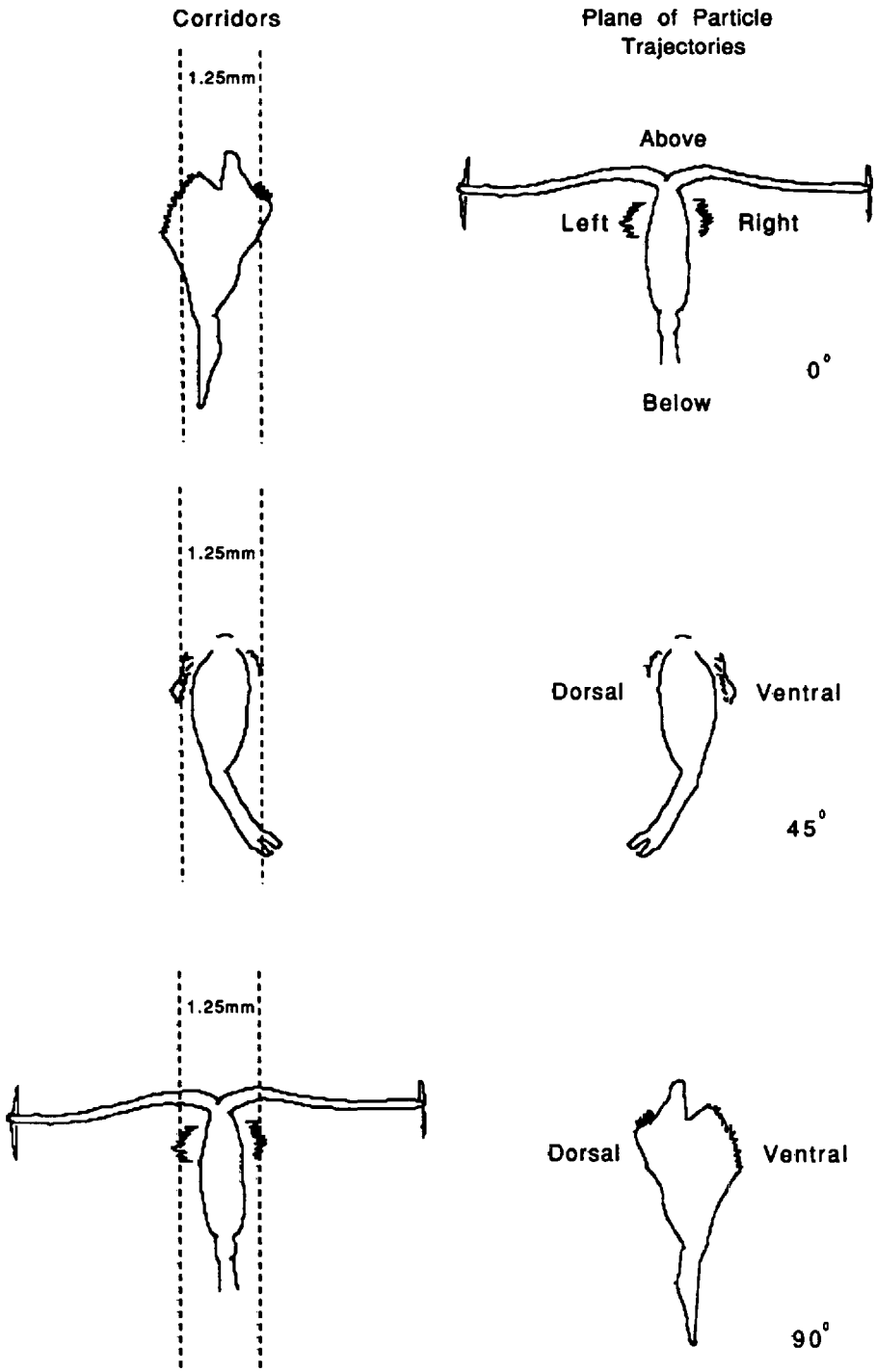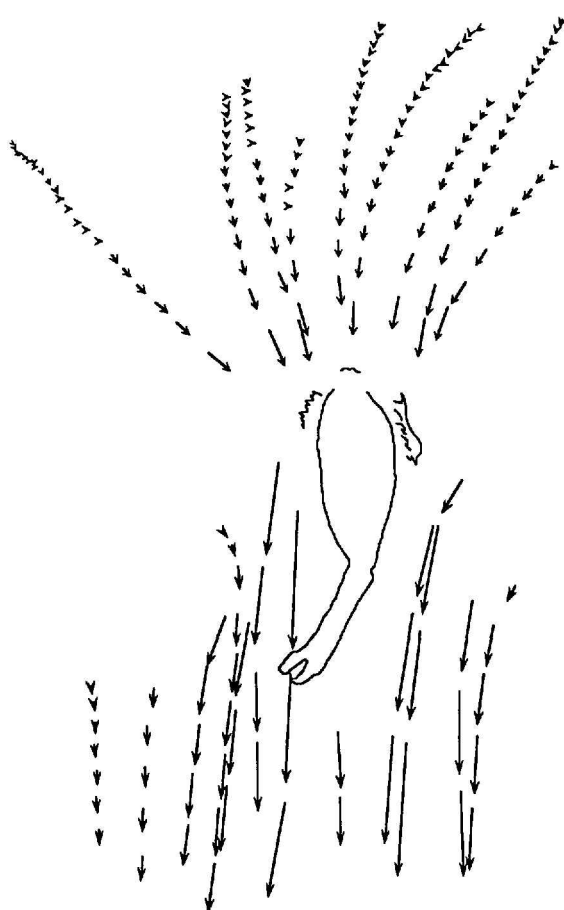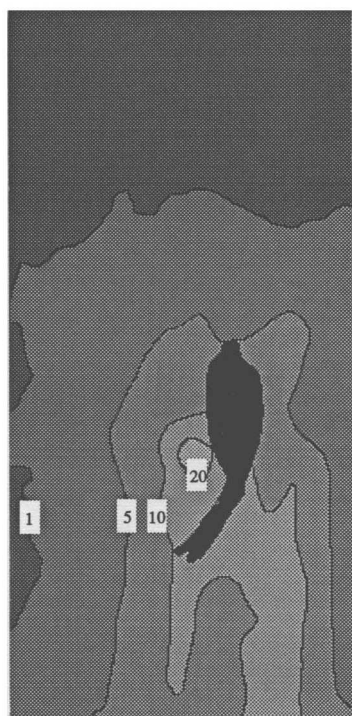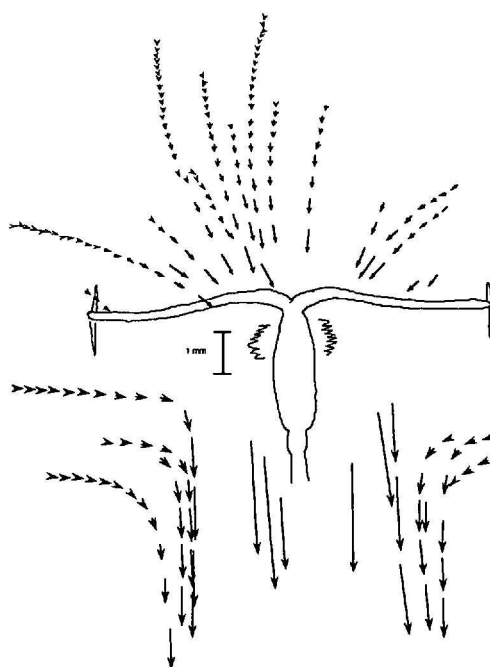
Figure 2. Corridors used in the analysis of the velocity isopleths and particle trajectories for the dorsal view (A), 45 degree view (B) and lateral view (C) of *Pleuromamma xiphias*.
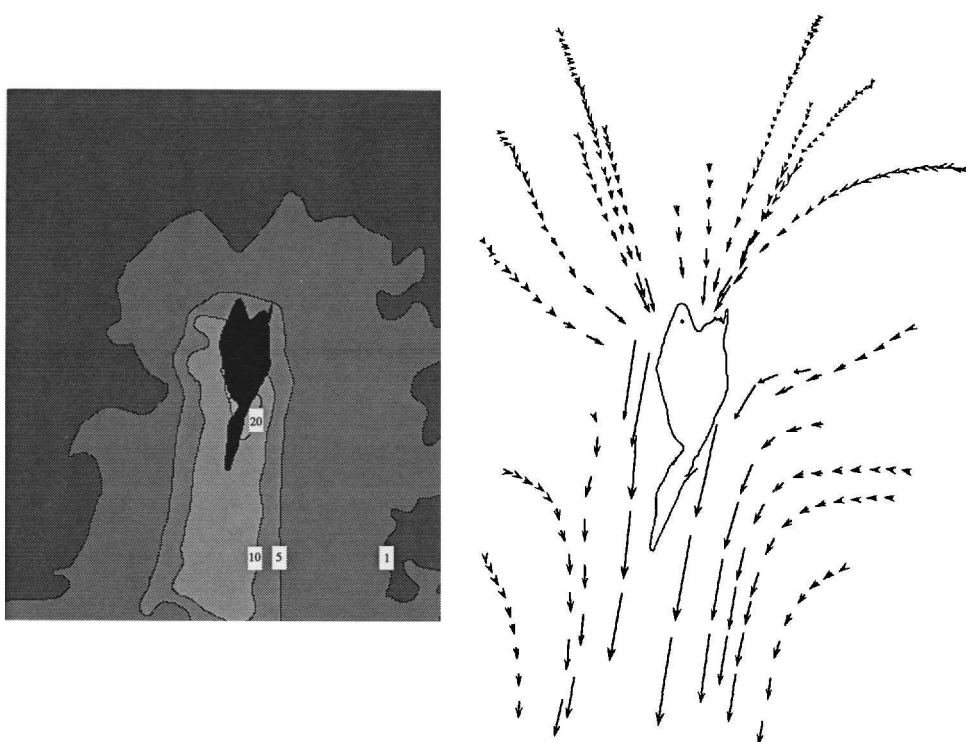
Figure 3E. Velocity isopleths—lateral view. Legend same as Figure 3A. Figure 3F. Particle trajectories—lateral view. Legend the same as Figure 3A.

found proximal to the animal. Results of the velocity profile of three individuals of the same sex and age class are shown in this figure.

Water velocity profiles of the lateral view (Fig. 5) show asymmetry between the dorsal and ventral region of the animal with the velocity isopleths in both the 45 degree view (Fig. 3C) and the lateral view (Fig. 3E) extending further ventrally than dorsally from the body of the animal. Figure 6 shows the surface area enclosed by each of the velocity isopleths from 1.00–5.00 mm·s^{-1} on a plane defined by the top of the antennae. The area multiplied by the magnitude of the velocity describes the flux of water through each region. Again the disproportionate amount of water which approaches ventral to the animal is apparent.

Below the First Antennae.—Below the antennae the structure of the flow field becomes more spatially volatile with isolated regions of high velocity. The highest velocity recorded was 38.00 mm·s^{-1}, found lateral to the animal (Fig. 3A). The

←

Figure 3.   Velocity isopleths and particle trajectories. Velocity isopleths and particle trajectories for *Pleuromamma xiphias* from a dorsal view (A and B), 45 degree view (C and D), and lateral view (E and F). For velocity isopleths decreased shading corresponds to increased flow magnitude. Selected isopleths are labeled in units of mm·sec^{-1}. Length of arrows in particle trajectories represent distance traveled in ⅙ s. Figure 3B. Particle trajectories—dorsal view. Legend same as Figure 3A.

Figure 3C. Velocity isopleths–45 degree view. Legend same as Figure 3A. Figure 3D. Particle trajectories—45 degree view. Legend same as Figure 3A.
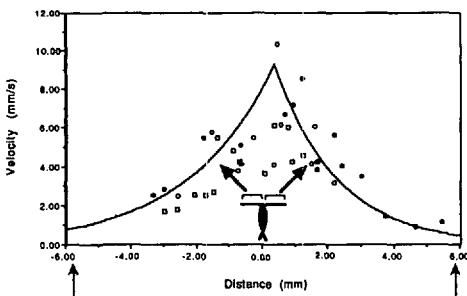
Figure 4 (left). Profile of the water velocity along the first antennae of *Pleuromamma xiphias*. Increasing negative values represent distance traveled toward the distal tip along the left antennae while positive values are the distances traveled along the right antennae. Symbols represent data taken from three different animals. The curve is an exponential fit to data derived from contour. Arrows indicate distal tips of the antennae.
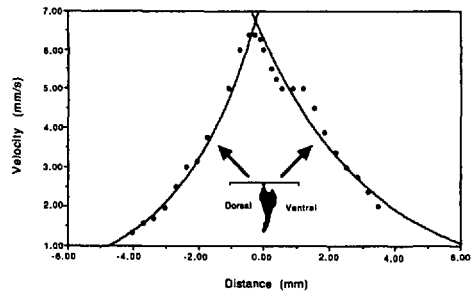
Figure 5 (right).   Profile of the water velocity perpendicular to the first antennae of *Pleuromamma xiphias*. Graph uses data derived from the contoured velocities. Increasing negative values represent distance traveled away from the animal dorsally, while positive values are the distances traveled ventrally away from the body. Data was fit to an exponential curve.

lateral dimension of the volume of water traveling at this velocity must be less than one body width since it was only marginally detected in the lateral view (Fig. 3E). A region of high velocity was also detected dorsal to the animal just below the level of the antennae (Fig. 3E). Below the animal, the extent of the hydrodynamic disturbance defined by the outer most velocity isopleth (1.00 mm·s^{-1}) was not detected using the field of view available with the present equipment; however, water velocities decreased to the 7.00 mm·s^{-1} isopleth at 7.50 mm below the top of the head. Interesting to note is the continuous intrusion of water and particles in the region below the first antennae and feeding appendages (Fig. 3B, D, F). This lateral entrainment arises as a result of the preservation of the total momentum of the system. As the water is thrust away from the flow generating appendages, a small portion of the momentum of the water is lost heat. However, the majority of the total energy accelerates the surrounding water mass which results in the lateral entrainment of water (Tritton, 1982).

DISCUSSION

Our objectives in this study were to propose a new method for the analysis of feeding current and to use this method to describe the nature of the hydrodynamic disturbance of the feeding current of *Pleuromamma xiphias*. Two types of disturbances are produced when an object moves through a fluid; a pressure wave which involves the movement of energy traveling at the speed of sound and only a relatively small water displacement, and an actual fluid displacement which involves the movement of a water mass. Because of the small size of the appendages and the frequency at which they beat, use of the created pressure wave is an ineffective means of detecting a potential prey (Kirk, 1985). Therefore, Kerfoot (1978) suggests fluid displacement as the major characteristic of the flow used by mechanoreceptive predatory copepods to detect their prey. Herein we used particle trajectories as a measure of the net flow velocity that represents the actual water displacement rather than the pressure wave generated by the flow current of the animal.

Dorsal

Right Antennae   **Left Antennae**

5.00 +
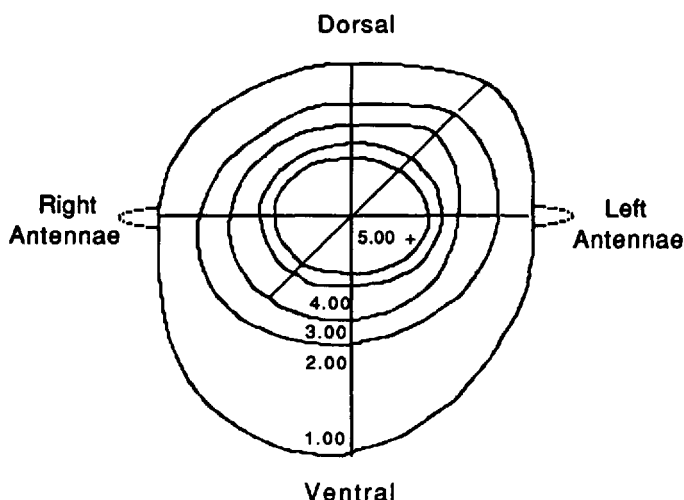
4.00
3.00
2.00

1.00

Ventral

Figure 6.   Water velocity through the antennal plane. A cross section of the flow field of *Pleuromamma xiphias* defined by the plane perpendicular to the body of the animal encompassing the first antennae. Values shown are in units of mm·s⁻¹.

Feeding Current Analysis. — Our methods as presented in this study worked well to track particles within a narrow volume. The accurate depiction of the laminar flow suggests that the size of the corridor chosen is in general adequate for this type of analysis. However, a problem region is apparent when comparing the velocity profiles in the dorsal (Fig. 4) and the lateral (Fig. 5) view directly above the head. The values in the two graphs should be identical because they represent the same 3-dimensional point. The inconsistency in the values can be explained by the exponential decrease in velocity profiles. An analysis using a corridor of even a minimum volume in the proximal region of the antennae will be subject to error as a result of the rapid deceleration in velocity over small distances. Using the present corridor size a maximum error in projecting a gradient of different velocities on to a defined plane is equal to the difference between the maximum flow region, in this case above the head of the animal, and the edge of the corridor. This compression of trajectories can give rise to approximately a 20% error for the most rapid flow regions. A thinner corridor would diminish this error. The size of the corridor used was an effort to balance the large number of trajectories needed for this type of analysis with the uncertainty of the stability of the flow field over time. Use of a narrow corridor decreases the number of particles which can be plotted traveling in the plane of interest, while a wide corridor loses the accuracy by compressing a large volume onto the same plane.

The similarity between the water velocity profile taken for three different animals suggests that there is both temporal stability within each animal and morphological stability between individuals of the same sex and age class of this species. Since there is temporal stability of the flow field, then more than a single 2-h tape can be used in an analysis. In addition, depending on the desired resolution, a very narrow corridor could be used.

The size of the filming vessel (125 cm³) was considerably larger than the dimensions of the flow fields. Therefore, any container effect on the shape and velocity of the feeding current is presumed to be minimal (Fig. 7). The effect of
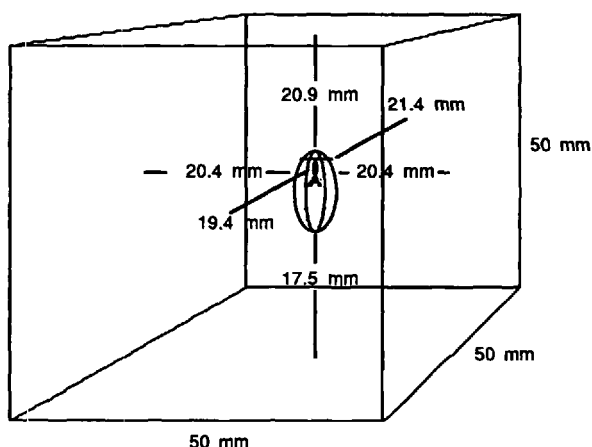
Figure 7.   Dimensions of flow field. The dimensions of the flow field defined by the 1.00-mm isopleth with respect to the size of the filming container.

being tethered on the characteristics of the flow field is not explored in this study. However, when the animal is moving the absolute magnitudes of the water velocities would be expected to be less than those found here since some of the energy used to generate the feeding current will be used to sustain the swimming motion of the animal and overcome the effect of drag.

Feeding Current Morphology. — In describing the flow over the antennae, Strickler (1985) suggests three general regions of flow: a motion core, a viscous core and sensory core. This study shows a fourth region surrounding the motion core: the distal shell, located at the distal tip of the first antennae where the water velocity approaches background levels. It is in this region that the mechanoreceptive setae on the distal tip of the antennae may be able to detect an external hydrodynamic signal whose intensity is greater than the self-generated disturbance within the flow field (Lenz and Yen, 1993). Here, we arbitrarily use the $1 \text{ mm} \cdot \text{s}^{-1}$ isopleth to enclose the flow field. The $1.00 \text{ mm} \cdot \text{s}^{-1}$ was measured as far as 4.10 mm above the head, 4.60 mm laterally, 5.60 mm ventrally and 3.60 mm dorsal to the animal. The lower extent of the $1.00 \text{ mm} \cdot \text{s}^{-1}$ isopleth was not shown because it was not within the field of view; however, the $7.00 \text{ mm} \cdot \text{s}^{-1}$ velocity isopleth was found 7.50 mm directly below the head. Using the above dimensions and a spheroid model based on geometric averages of the different values (due to the asymmetry in the flow field), the volume of the hydrodynamic distrubance (approximately 4 mL) created by the animal is greater than 175 times the actual volume of the physical body of the animal. This calculation is a conservative estimate of the outer extent of the flow field since neurophysiological data suggest that the animal can detect velocities as low as $20 \mu \text{m} \cdot \text{s}^{-1}$ (Yen et al., 1991). Therefore, by creating a feeding current, the animal incurs an evolutionary cost: the animal becomes more "visible" to its mechanoreceptive predators and the feeding current acts as an indicator of the animal's identify (Strickler and Twombly, 1975; Kirk, 1985) and gives away its location to its predators. We also must recognize that individual species of organisms behaviorally assessing the flow field may sense velocity or only a portion of the characteristics of the flow [i.e., change in velocity over time or a particular distance, rate-of-strain tensor or vorticity tensor (Yen et al., 1991; Zaret, 1981)]. Without a solid foundation in the sensory capabilities of interacting

organisms it is difficult to gain insight into how organisms "view" each other. Studies which integrate information from neurophysiological and behavioral studies are necessary to fill the present gap in understanding the interactions between aquatic mechanoreceptive organisms.

In general, symmetry between the left and right side of the animal was observed as was reported by Paffenhöfer and Lewis (1990). This differs from the reports of asymmetry found in the feeding current of *E. crassus* (Koehl and Strickler, 1981). The likely reason for this is because the feeding current reported in this paper is averaged over half an hour while Koehl and Strickler (1981) describe a flow field generated over a much shorter time frame. Therefore they recorded a particular behavioral event in which the animal had re-routed an individual particle's trajectory.

During the filming, motion was observed in both the 2nd antennae and the 2nd maxillae. However, from observations of appendage motion the feeding current seems to be primarily caused by the movement of the 2nd antennae. The areas of highest velocity are found to the left and right of the animal associated with the downward swing of the 2nd antennae. Dorsal to the animal (Fig. 3C), slightly below the level of the antennae, is a second region of high velocity also associated with the motion of the 2nd antennae. The two separate regions of high velocity are a result of the biramous nature of the 2nd antennae. Due to the low Reynolds number (less than 100) at which this flow is operating, some reversal of the flow would be expected if the appendages were to be simply pulled back up. However, particle trajectories did not indicate any flow reversal in the upswing. A possible explanation for this is that the orientation of the appendages may change with the up and downward stroke.

Asymmetry in the dorsal and ventral flow was detected with the majority of the water approaching from above and ventral to the animal. The asymmetry in the flow field was most pronounced in the low flow regions below $1.00 \text{ mm} \cdot \text{s}^{-1}$ isopleth which acocunts for only a small fraction of the total volume of water entrained by the animal. However, in terms of the hydrodynamic disturbance, the asymmetrical shape of the flow field creates higher velocity gradients dorsal to the animal while the lower values are located ventral to the animal. Since the magnitude of the velocity gradient has been implicated as the most probable characteristic of the hydrodynamic signal eliciting an escape response, the lower values found ventral to the animal, depicted by the more sparsely spaced velocity contours, may decrease the distance at which the prey can detect the predator. Therefore, the prey entrained ventral to the predator would approach closer to the capture region before initiating an escape response than if they were entrained dorsal to the predator.

The small fraction of water entrained in the low flow regions, both dorsal and ventral to the animal, do not pass over the sensors located on the first antennae. Since the flow is laminar, chemical signals emitted by prey (particulate or motile prey) in this region, cannot be detected by the 1st antennae and may have to be assessed by the sensors located on the feeding appendages themselves. Mechanical stimuli, however, can be transmitted across streamlines and are not restricted to the predetermined trajectories defined by the laminar lines (Tiselius and Jonsson, 1990). Therefore the mechanical stimuli generated in this region may be detected by the numerous mechanoreceptors located on the first antennae of most copepods (Gill, 1986; Yen and Nicoll, 1990; Yen et al., 1991).

Since the feeding current may be a major constituent governing the interaction between an animal and its predators and prey, it seems likely that the shape and magnitude of the hydrodynamic disturbance is under strong evolutionary pressure.

Differences in diet may be reflected in fine scale adaptations in the morphology of the feeding current in the same manner as they are mirrored in the swimming behavior (Buskey, 1984) and the morphology of the mouth parts (Itoh, 1970) in the different copepod species. Regions in which there is intensive predation by mechanoreceptive organisms may give rise to prey which create smaller feeding currents. On the opposite end of the spectrum, if food quantity is a major evolutionary driving force then feeding currents may be relatively large to entrain more water which would be scanned or passed over the feeding appendages. It also is possible that there exists individual phenotypic plasticity in the shape and magnitude of flow field as a result of exposure to different particle concentrations, size or prey type. The latter may help explain the observations of switching of predation pressures from one prey type to another when concentrations go below a critical value (Landry, 1981).

ACKNOWLEDGMENTS

LITERATURE CITED

Ambler, J. W. and C. B. Miller. 1987. Vertical habitat-partitioning by adults of subtropical oceanic copepods. Mar. Biol. 94: 561–577.
Bennett, J. L. and T. L. Hopkins. 1989. Aspects of the ecology of the calanoid copepod genus *Pleuromamma* in the eastern Gulf of Mexico. Contri. Mar. Sci. 31: 119–136.
Buskey, E. J. 1984. Swimming patterns as an indicator of the roles of copepods sensory systems in the recognition of food. Mar. Biol. 78: 53–57.
———, K. S. Baker, R. C. Smith and E. Swift. 1989. Photosensitivity of the oceanic copepods *Pleuromamma gracilis* and *Pleuromamma xiphias* and its relationship to light penetration and daytime depth distribution. Mar. Ecol. Prog. Ser. 55: 207–216.
Cannon, H. G. 1928. On the feeding mechanisms of the copepods *Calanus finimarchicus* and *Diaptomus gracilis*. J. Exp. Biol. 6: 131–144.
Foxton, P. and H. S. J. Roe. 1974. Observations on the nocturnal feeding of some mesopelagic decapod crustaceans. Mar. Biol. 28: 37–49.
Gilbert, J. J. and K. L. Kirk. 1988. Escape responses of the rotifer *Kertella*: description, stimulation, fluid dynamics and ecological significance. Limnol. Oceanogr. 33: 1440–1450.
Gill, C. W. 1986. Suspected mechano and chemosensory structures of *Temora longicornis* (Copepoda: Calanoida). Mar. Biol. 93: 449–457.
Haury, L. R. 1988. Vertical distribution of *Pleuromamma* (Copepoda: Metridinidae) across the eastern North Pacific Ocean. Hydrobiologia 167/168: 335–342.
———, D. E. Kenyon and J. R. Brooks. 1980. Experimental evaluation of the avoidance reaction of *Calanus finimarchicus*. J. Plankt. Res. 2: 187–202.
Hopkins, T. L. and R. C. Baird. 1981. Trophodynamics of the fish *Valenciennellus tripunculatus*. I. Vertical distribution, diet and feeding chronology. Mar. Ecol. Prog. Ser. 5: 1–10.
——— and ———. 1985. Aspects of the trophic ecology of the mesopelagic fish *Lampanyctus alatus* (Family Myctophidae) in the eastern Gulf of Mexico. Biol. Oceanogr. 3: 285–313.
Hu, V. J. H. 1978. Relationships between vertical migration and the diet in four species of euphasiids. Limnol. Oceanogr. 23: 296–306.
Itoh, K. 1970. A consideration on the feeding habits of planktonic copepods in relation to the structure of their oral parts. Bull. Plankton Soc. Japan 17: 1–10.
Kerfoot, W. C. 1978. Combat between predatory copepods and their prey: *Cyclops, Episcura* and *Bosmina*. Limnol. Oceanogr. 23: 1089–1102.
Kirk, K. L. 1985. Water flow produced by *Daphnia* and *Diaptomus*: implications for prey selection by mechanosensory predators. Limnol. Oceanogr. 30(1): 679–686.

Kitalong, A. 1988. Diel variation in composition and abundance of a deep-water zooplankton community in Hawaii, with some aspects of their feeding and reproductive biology. M.S. Thesis, University of Hawaii at Manoa. 67 pp.

Koehl, M. A. R. and J. R. Strickler. 1981. Copepod feeding currents: food capture at low reynolds numbers. Limnol. Oceanogr. 26: 1062–1073.

Landry, M. M. 1981. Switching between herbivory and carnivory by the planktonic marine copepod, *Calanus pacificus*. Mar. Biol. 67: 77–82.

Lenz, P. H. and J. Yen. 1993. Distal setal mechanoreceptors of the first antennae of marine copepods. Bull. Mar. Sci. 53: 170–179.

Mullin, M. M. 1966. Selective feeding by calanoid copepods from the Indian Ocean. Pages 545–554 *in* H. Barnes, ed. Some contemporary studies in marine science. George Allen and Unwin Ltd., London.

Paffenhöfer, G-A. and Lewis, K. 1990. Perceptive performance and feeding behavior of calanoid copepods. J. Plankt. Res. 12(5): 993–946.

Strickler, J. R. 1985. Feeding currrents in calanoid copepod: two new hypotheses. Pages 459–485 *in* M. S. Laverack, ed. Physiological adaptations of marine animals. Soc. Exp. Biol. 89.

―――― and S. Twombley. 1975. Reynolds number, diapause, and predatory copepods. Verh. Int. Ver. Limnol. 619: 2948–2950.

Tiselius, P. and Per R. Jonsson. 1990. Foraging behavior of six calanoid copepods: observations and hydrodynamic analysis. Mar. Ecol. Prog. Ser. 66: 23–33.

Tritton, D. J. 1982. Physical fluid dynamics. Pages 112–119. Van Nostrand Reinhold (UK) Co. Ltd. 362 pp.

Yen, J. and D. M. Fields. 1993. Escape responses of *Acartia hudsonica* (Copepoda) nauplii from the flow field of *Temora longicornis* (Copepoda). Ergeb. Limnol. 36: 123–134.

―――― and N. T. Nicoll. 1990. Setal array on the first antennae of the carnivorous marine copepod, *Euchaeta norvegica*. J. Crust. Biol. 10: 218–224.

――――, B. Sanderson, J. R. Strickler and A. Okubo. 1991. Feeding current and energy dissipation by *Euchaeta rimana,* a subtropical pelagic copepod. Limnol. Oceanogr. 36: 362–369.

Zaret, R. E. 1981. Zooplankton and their interactions with water, with each other, and with their predators. Ph.D. Dissertation, John Hopkins Univ. 177 p.

ADDRESS: *Marine Sciences Research Center, State University of New York, Stony Brook, New York 11794-5000.*